

## New insights into the crystal chemistry of epididymite and eudidymite from Malosa, Malawi: A single-crystal neutron diffraction study

G. DIEGO GATTA,<sup>1,2,\*</sup> N. ROTIROTI,<sup>1,2</sup> G.J. MCINTYRE,<sup>3</sup> A. GUASTONI,<sup>4</sup> AND F. NESTOLA<sup>4</sup>

<sup>1</sup>Dipartimento di Scienze della Terra, Università degli Studi di Milano, Via Botticelli 23, I-20133 Milano, Italy

<sup>2</sup>CNR-Istituto per la Dinamica dei Processi Ambientali, Milano, Italy

<sup>3</sup>Institut Laue-Langevin, BP 156, 38042 Grenoble Cedex 9, France

<sup>4</sup>Dipartimento di Geoscienze, Università degli Studi di Padova, Italy

### ABSTRACT

The crystal chemistry of two dimorphic hydrated sodium beryllium silicates, epididymite [ $a = 12.7334(4)$ ,  $b = 13.6298(5)$ ,  $c = 7.3467(3)$  Å,  $V = 1275.04$  Å<sup>3</sup>, space group  $Pnma$ ] and eudidymite [ $a = 12.6188(10)$ ,  $b = 7.3781(5)$ ,  $c = 13.9940(9)$  Å,  $\beta = 103.762(5)^\circ$ ,  $V = 1265.47$  Å<sup>3</sup>, space group  $C2/c$ ] from Malosa, Malawi, has been reinvestigated by means of energy dispersive X-ray spectroscopy, thermo-gravimetric analysis, inductively coupled plasma-optical emission spectroscopy and single-crystal neutron diffraction. Two anisotropic structure refinements have been performed with final agreement index  $R_1 = 0.0317$  for 137 refined parameters and 2261 unique reflections with  $F_o > 4\sigma(F_o)$  for epididymite, and  $R_1 = 0.0478$  for 136 refined parameters and 1732 unique reflections with  $F_o > 4\sigma(F_o)$  for eudidymite. The analysis of the difference-Fourier maps of the nuclear density of the two dimorphs confirms the presence of extra-framework water molecules in both, and not hydroxyl groups as wrongly reported in previous studies and in several crystal-structure databases. The correct chemical formula of epididymite and eudidymite is  $\text{Na}_2\text{Be}_2\text{Si}_6\text{O}_{15} \cdot \text{H}_2\text{O}$  ( $Z = 4$ ). The configuration of the water molecules and the hydrogen bonds are fully described for both the dimorphs. The chemical analyses show that a small, but significant, amount of Al and Fe (most likely substituting for Si in the tetrahedral sites) and K (substituting for Na as an extra-framework cation) occurs in both dimorphs.

**Keywords:** Epididymite, eudidymite, crystal chemistry, single-crystal neutron diffraction, hydrogen bonding

### INTRODUCTION

Epididymite and eudidymite are dimorphous open-framework silicate minerals, with a poorly defined ideal chemical formula (i.e.,  $\text{Na}_2\text{Be}_2\text{Si}_6\text{O}_{15} \cdot \text{H}_2\text{O}$ , Fang et al. 1972;  $\text{NaBeSi}_3\text{O}_7\text{OH}$ , Robinson and Fang 1970; the *American Mineralogist* Crystal Structure Database, Downs and Hall-Wallace 2003).

The original description of eudidymite was given by Brøgger (1890) on specimens from Norway, whereas the first description of epididymite was given by Flink (1894) on specimens from Greenland (presumably from the Narssârssuk pegmatite). Epididymite and eudidymite have been found in many localities worldwide. Among those, the most significant include the Narssârssuk pegmatite and the Illimaussaq complex in Greenland (Lévy 1961; Petersen 1966), Věžná in the Czech Republic (Černý 1963), the Kola Peninsula in Russia (Shilin and Semenov 1957), Montana St. Hilaire and Seal Lake in Canada (Nickel 1963; Mandarino and Harris 1968), and several localities in Norway (Brøgger 1890). Both of these minerals occur as late-stage minerals in the cavities of alkaline pegmatites generally associated with aegirine, Na-feldspars, zeolites, and many other rare, exotic minerals including Na-Be-Zr-Y silicates, Nb-Ta oxides, and REE-carbonates.

The crystal structure of epididymite was first solved by Ito

(1934) and then re-investigated by Pobedimskaya and Belov (1960). However, a further re-investigation by Robinson and Fang (1970), by means of single-crystal X-ray diffraction with Buerger precession photographs, showed that the structure models previously published were wrong. The authors refined the crystal structure of epididymite in space group  $Pnma$ , with  $a \sim 12.74$ ,  $b \sim 13.63$ , and  $c \sim 7.33$  Å, giving two possible chemical formulas,  $4(\text{NaBeSi}_3\text{O}_7\text{OH})$  or  $4(\text{Na}_2\text{Be}_2\text{Si}_6\text{O}_{15} \cdot \text{H}_2\text{O})$ , due to the conflicting results about the presence of water molecules or hydroxyl groups. The crystal structure of epididymite contains  $[\text{Si}_6\text{O}_{15}]_\infty$  double chains of  $\text{SiO}_4$  tetrahedra, running parallel to  $[001]$  (Fig. 1). The silicate chains are joined by two edge-sharing  $\text{BeO}_4$  tetrahedra, with a topological configuration shown in Figure 1. In other words, Si and Be tetrahedra represent the “framework” of this crystal structure. The “extra-framework” Na site shows an irregular sevenfold coordination. Despite the general structure model of Robinson and Fang (1970) being quite plausible, as shown by bond distances and angles, the authors were not able to refine the anisotropic displacement factors of the atomic sites and, in addition, were not able to locate the proton site(s), leaving an open question concerning the topological configuration of the water molecule, or hydroxyl group, and the relationship between the extra-framework (i.e.,  $\text{Na} + \text{H}_2\text{O}$ ) and framework content, especially the role played by the H-bonds. In addition, the agreement factor reported by the authors is high ( $R_1 \sim 8.4\%$ ).

\* E-mail: diego.gatta@unimi.it

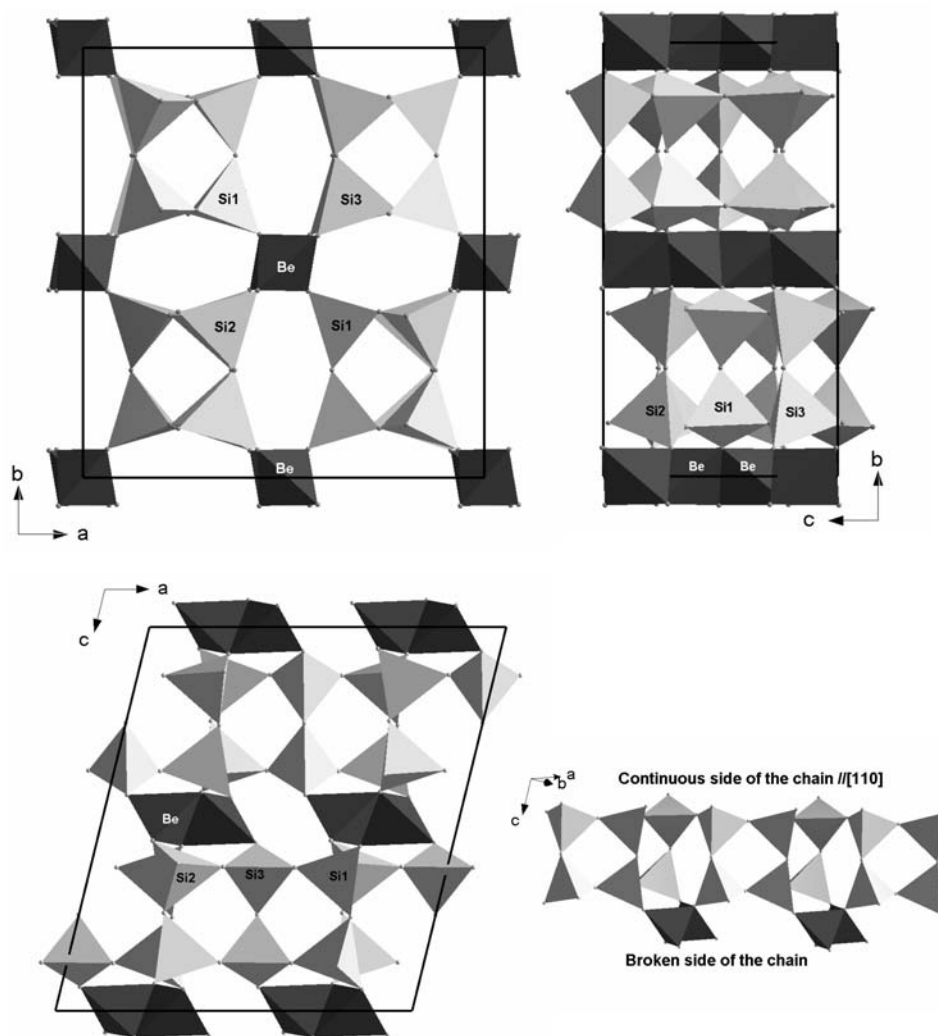


FIGURE 1. The tetrahedral frameworks of (above) epididymite and (below) eudidymite. Beryllium tetrahedra are in dark gray, Si tetrahedra in light gray.

The crystal structure of eudidymite was first reported by Ito (1947) and then re-investigated by Fang et al. (1972). The latter authors described the crystal structure of eudidymite in space group  $C2/c$  with  $a \sim 12.62$ ,  $b \sim 7.38$ ,  $c \sim 14.02$  Å,  $\beta \sim 103.72^\circ$ , with ideal chemical formula  $\text{Na}_2\text{Be}_2\text{Si}_6\text{O}_{15} \cdot \text{H}_2\text{O}$  ( $Z = 4$ ) (Fang et al. 1972). The structure of eudidymite consists of infinite chains, made up by  $\text{SiO}_4$  tetrahedra running along  $[110]$ , which form sheets parallel to  $(001)$ . The aforementioned sheets are cross-linked by edge-sharing  $\text{Be}_2\text{O}_6$  units, to form a 3-dimensional framework. The eminent  $\{001\}$  cleavage of eudidymite is mainly due to the orientation of the double-sheets of  $\text{SiO}_4$  units. The extra-framework Na site is sevenfold coordinated to six O atoms belonging to the tetrahedral framework and one water molecule or hydroxyl group (Fang et al. 1972).

The relationship between the structures of epididymite and eudidymite can be intuitively understood from Figure 1. In epididymite, the double chains are bonded only through  $\text{Be}_2\text{O}_6$  units (and Na atoms). Any given  $\text{Be}_2\text{O}_6$  unit is bonded to all the four double chains present in the unit cell. In contrast, in eudidymite, one chain, which extends along  $[110]$  and is made up

of  $\text{SiO}_4$  units, is continuous, whereas the second one is broken at every third shared oxygen to accommodate a cross-linking  $\text{Be}_2\text{O}_6$  unit (Fig. 1). In other words, in the eudidymite framework real “double chains” made up only of  $\text{SiO}_4$  units do not exist; however, this term is currently used in the literature (Fang et al. 1972). For eudidymite, just as for epididymite, Fang et al. (1972) provided only structural data based on an isotropic refinement, without any information about the location of the proton sites and the role played by the H bonds. Also in this case, the agreement factor reported by the authors is high ( $R_1 \sim 8.0\%$ ).

In this light, the aim of the present study is a reinvestigation of the crystal structures and crystal chemistry of natural epididymite and eudidymite at ambient conditions by means of energy dispersive X-ray spectroscopy, thermo-gravimetric analysis, inductively coupled plasma-optical emission spectroscopy, and single-crystal neutron diffraction to define: (1) the real chemical formula of these minerals; (2) the location of the proton site(s), and the real topological configuration of the water molecules or hydroxyl groups, to obtain a full description of the relationship between framework and extra-framework content (e.g., via H

bonds); and (3) the anisotropic displacement parameters of all the atomic sites. Since the X-ray diffraction studies have proven to be insufficient to locate directly the (possibly disordered) H atoms, single-crystal neutron diffraction represents the only experimental technique that allows one to answer the open questions about the crystal chemistry of these two dimorphs.

### SAMPLES DESCRIPTION AND MINERALOGY

Two natural samples of euidymite and epididymite, collected from a miarolitic granitic pegmatite hosted by A-type peralkaline granites (Martin and De Vito 2005) of the Zomba-Malosa pluton in southern Malawi, were selected for the experiments in the present study. The Zomba-Malosa pluton, emplaced ~113 My, is composed of qz-syenite and peralkaline granite and belongs to the Chilwa-alkaline province of Cretaceous age (Eby et al. 1995). These pegmatite bodies are subhorizontal, strongly miarolitic, and contain cavities decimeters to meters in size. These cavities host an exotic mineralogy that includes aegirine, arfvedsonite, fluorite, quartz, K-feldspar, niobophyllite, xenotime-(Y), zircon, and many exotic phases like REE-carbonates, Nb-Ta-Y-Th oxides, Be-Na-Zr-Ba silicates, and Be-Y silicates. A description of some pegmatite minerals from the Zomba district is in Petersen (1994). A recent structure investigation by single-crystal X-ray diffraction on aegirine in the cavities from Mount Malosa indicates that the crystallization occurred at ~1 kbar and at temperature of 300–400 °C (Secco et al. 2007).

The euidymite samples from the Zomba-Malosa pluton show large, white, opaque crystals, tabular on (001), pseudo-rhombic in shape, up to 5 cm in length and a few millimeters in thickness; cleavage on (001) is perfect. The epididymite crystals are large, white and partially transparent, tabular on (001) and prismatic in shape, up to 4 cm in length and several millimeters in thickness; (001) cleavage is perfect. Large single crystals of epididymite and euidymite were selected for the chemical analysis and for the neutron diffraction experiments.

### EXPERIMENTAL METHODS

Quantitative electron microprobe analyses were performed on polished samples of epididymite and euidymite using a JEOL 5610 LV scanning electron microscope equipped with a Gresham energy dispersive X-ray spectrometer (SEM-EDS) at the Museum of Natural History of Milan. The system was operated with an accelerating voltage of 20 kV, filament current of 85  $\mu$ A, beam diameter of 2  $\mu$ m, and counting time of 60 s per point analysis. Natural crystals of albite and orthoclase (for Si, Al, K, Na, and Ca) and synthetic alloys (for Fe) were used as standards. The results were processed for matrix effects by a conventional ZAF routine included in the Gresham analysis package. The crystals were found to be homogeneous within the analytical error. Beryllium content was determined by inductively coupled plasma-optical emission spectroscopy (ICP-OES) using a Liberty 220 Varian instrument and H<sub>2</sub>O content was determined by thermo-gravimetric (TG) analysis using a Netzsch 490 instrument, both performed at the Mapei SpA Laboratories in Milan, Italy. The final chemical formulas of epididymite and euidymite are reported in Table 1.

The crystals of epididymite and euidymite selected for the neutron diffraction study were plates of dimensions 4 × 3 × 0.8 and 5 × 2 × 0.2 mm<sup>3</sup>, respectively (Table 2), and twinning-free (Petersen et al. 1997). Neutron-diffraction data for both compounds were measured at room temperature on the four-circle diffractometer D9 at the Institut Laue-Langevin, Grenoble, with a beam of wavelength 0.8362(2) Å obtained by reflection from a Cu (220) monochromator. D9 is equipped with a small two-dimensional area detector (Lehmann et al. 1989), which for this measurement allowed optimal delineation of the peak from the background. Most reflections of the type  $-h, \pm k, +l$  to  $\sin\theta/\lambda=0.80 \text{ \AA}^{-1}$  were scanned for epididymite to give two equivalents for each unique reflection, while an almost complete set of unique reflections of type  $-h, -k, \pm l$  to  $\sin\theta/\lambda=0.77 \text{ \AA}^{-1}$  was scanned for euidymite. A total

number of 4342 and 2707 reflections were collected for the structural refinements of epididymite and euidymite, respectively (Table 2). For all data, background corrections following Wilkinson et al. (1988) and Lorentz corrections were applied. Absorption corrections were made by Gaussian integration (Coppens et al. 1965) using the calculated attenuation coefficients  $\mu = 0.0490$  and  $0.0493 \text{ mm}^{-1}$ , for epididymite and euidymite, respectively, taking into account the wavelength dependence of the absorption for hydrogen (Howard et al. 1987), to give transmission ranges of 0.936–0.981 and 0.952–0.995. After corrections, the discrepancy factors among the symmetry related reflections were  $R_{\text{int}} = 0.0193$  (Laue class *mmm*) for epididymite and  $R_{\text{int}} = 0.0387$  (Laue class *2/m*) for euidymite.

**TABLE 1.** Representative compositions of epididymite (EPI) and euidymite (EUD) from Mount Malosa, Zomba, Malawi, based on SEM-EDS, ICP-OES, and TG analyses

wt%	EPI	EUD
Na <sub>2</sub> O	11.16(35)	11.40(38)
K <sub>2</sub> O	0.45(9)	0.49(7)
BeO	10.10(15)	10.15(17)
CaO	0.05(2)	0.06(2)
Fe <sub>2</sub> O <sub>3</sub>	0.13(6)	0.11(5)
Al <sub>2</sub> O <sub>3</sub>	0.34(9)	0.30(8)
SiO <sub>2</sub>	73.20(36)	73.10(41)
H <sub>2</sub> O	4.05(2)	3.81(3)
Total	99.48	99.42

Formula proportions based on 15 O atoms		
Na	1.778	1.815
K	0.047	0.051
Ca	0.004	0.005
$\Sigma$	1.829	1.871
Be	1.993	2.002
$\Sigma$	1.993	2.002
Si	6.014	6.003
Al	0.033	0.029
Fe <sup>3+</sup>	0.008	0.007
$\Sigma$	6.055	6.039
H <sub>2</sub> O	1.110	1.043

**TABLE 2.** Details of neutron data collection and refinement of epididymite and euidymite

	Epididymite	Euidymite
Crystal shape	Rectangular plate	Rectangular plate
Crystal size (mm <sup>3</sup> )	4 × 3 × 0.8	5 × 2 × 0.2
Crystal color	Translucent white	Translucent white
Unit-cell constants	$a = 12.7334(4) \text{ \AA}$ $b = 13.6298(5) \text{ \AA}$ $c = 7.3467(3) \text{ \AA}$ – $V = 1275.04 \text{ \AA}^3$	$a = 12.6188(10) \text{ \AA}$ $b = 7.3781(5) \text{ \AA}$ $c = 13.9940(9) \text{ \AA}$ $\beta = 103.762(5)^\circ$ $V = 1265.47 \text{ \AA}^3$
Chemical formula	Na <sub>2</sub> Be <sub>2</sub> Si <sub>6</sub> O <sub>15</sub> ·H <sub>2</sub> O	Na <sub>2</sub> Be <sub>2</sub> Si <sub>6</sub> O <sub>15</sub> ·H <sub>2</sub> O
Space group	<i>Pnma</i>	<i>C2/c</i>
Z	4	4
T (K)	298	298
Radiation (Å)	0.8362(2)	0.8362(2)
Diffractometer	D9 four circle	D9 four circle
Data-collection method	$\omega$ - $\theta$ scans	$\omega$ - $\theta$ scans
Max. 2 $\theta$	86.14	80.16
	$-15 \leq h \leq 19$	$-18 \leq h \leq 6$
	$-21 \leq k \leq 18$	$-11 \leq k \leq 6$
	$0 \leq l \leq 12$	$-20 \leq l \leq 21$
No. measured reflections	4342	2707
No. unique reflections	2685	2246
No. unique refl. with $F_o > 4\sigma(F_o)$	2261	1732
No. refined parameters	137	136
$R_{\text{int}}$	0.0193	0.0387
$R_1$ (F) with $F_o > 4\sigma(F_o)$	0.0317	0.0478
$R_1$ (F) for all the unique reflections	0.0439	0.0750
$wR_2$ (F <sup>2</sup> )	0.0658	0.0991
Goof	1.066	1.047
Weighting Scheme: a, b	0.0224, 1.27	0.0282, 7.84
Residuals (fm/Å <sup>3</sup> )	+0.9/–0.8	+0.9/–0.9

Note:  $R_{\text{int}} = \Sigma |F_o^2 - F_o^2(\text{mean})| / \Sigma F_o^2$ ;  $R_1 = \Sigma (|F_o| - |F_c|) / \Sigma |F_o|$ ;  $wR_2 = \{ \Sigma [w(F_o^2 - F_c^2)^2] / \Sigma [w(F_c^2)] \}^{0.5}$ ,  $w = 1 / (\sigma^2(F_c^2) + (a^*P)^2 + b^*P)$ ,  $P = (\text{Max}(F_o, 0) + 2^*F_c) / 3$ .

Since the three-dimensional count distribution around each reflection was observed, the centroids of all scanned reflections could be found. Least-squares matching of the observed and calculated centroids of the 1559 strongest reflections for epididymite gave a metrically orthorhombic unit cell with  $a = 12.7334(4)$ ,  $b = 13.6298(5)$ , and  $c = 7.3467(3)$  Å. For eudidymite, 377 strongest reflections were centered giving a metrically monoclinic unit cell with  $a = 12.6188(10)$ ,  $b = 7.3781(5)$ ,  $c = 13.9940(9)$  Å, and  $\beta = 103.762(5)^\circ$ . Other details pertaining to the data collections are listed in Table 2.

### STRUCTURE REFINEMENTS

The neutron diffraction data of epididymite were first processed with the program E-STATISTICS, implemented in the WinGX package (Farrugia 1999). This program carries out a Wilson plot, calculates the normalized structure factors ( $E$  values) and their statistics of distributions. The structure of epididymite was found to be centrosymmetric at 91.2% likelihood. Accordingly, the Sheldrick's  $|E^2 - 1|$  criterion (Sheldrick 1997) indicated that the structure is centrosymmetric ( $|E^2 - 1| = 0.999$ ). The intensity data were then processed with the program ASSIGN-SPACEGROUP (in WinGX, Farrugia 1999), which provides a valuable check on the supposed symmetry by comparing the equivalent reflections. Two possible space groups (both belonging to Laue class  $mmm$ ) were selected by the program:  $Pnma$

and  $Pn2_1a$ . However, the combined figure of merit (CFOM) showed unambiguously that space group  $Pnma$  is highly likely (CFOM- $Pnma = 0.658$ , CFOM- $Pn2_1a = 6.781$ ; the lower the value of CFOM, the more likely that the assignment is correct). The crystal structure refinement was then performed in space group  $Pnma$  using the SHELX-97 software (Sheldrick 1997), with anisotropic thermal displacement parameters and starting from the atomic coordinates of Robinson and Fang (1970), without any H site. The neutron scattering lengths of Na, Be, Si, O, and H have been used according to the *International Tables for Crystallography C* (Wilson and Prince 1999). The secondary isotropic extinction effect was corrected according to the formalism of Larson (1970), as implemented in the SHELXL-97 package (Sheldrick 1997). When convergence was achieved, two intense negative residual peaks ( $\sim -13$  fm/Å<sup>3</sup>) at  $x \sim 0.006$ ,  $y = 1/4$ ,  $z \sim 0.586$  and  $x \sim 0.013$ ,  $y = 1/4$ ,  $z \sim 0.385$  were found in the final difference-Fourier map of the nuclear density (Fig. 2). A further refinement was then performed assigning H to these residual peaks, as hydrogen has a negative-neutron scattering length.

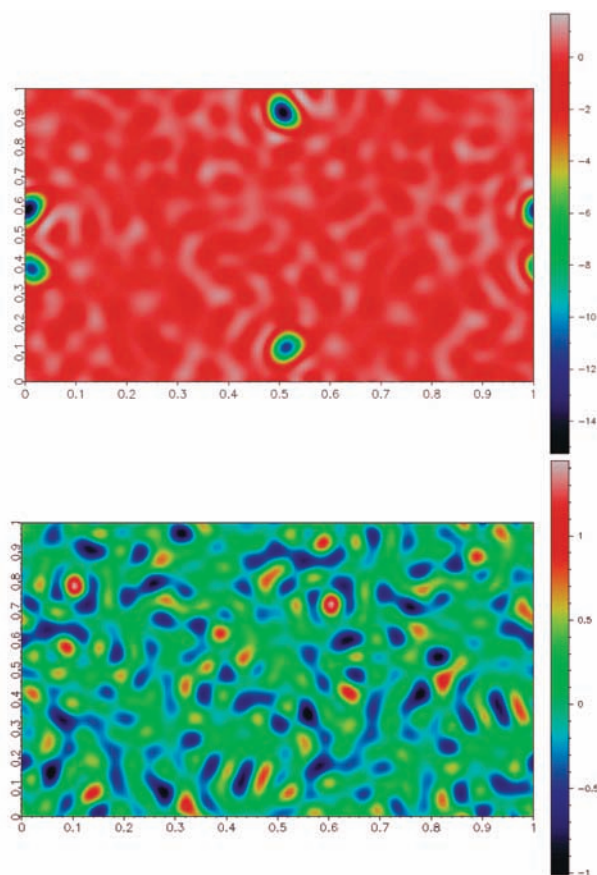


**FIGURE 2.** Difference Fourier maps of the nuclear density (fm/Å<sup>3</sup>) of epididymite at  $y = 1/4$  (above) after the first cycles of refinement without any H site, showing two intense negative residual peaks at  $x \sim 0.006$ ,  $z \sim 0.586$  and  $x \sim 0.013$ ,  $z \sim 0.385$ , and (below) after the assignment of the two H1 and H2 sites. Notes: the color scale is different for the two maps; map orientation: x positive to the right.

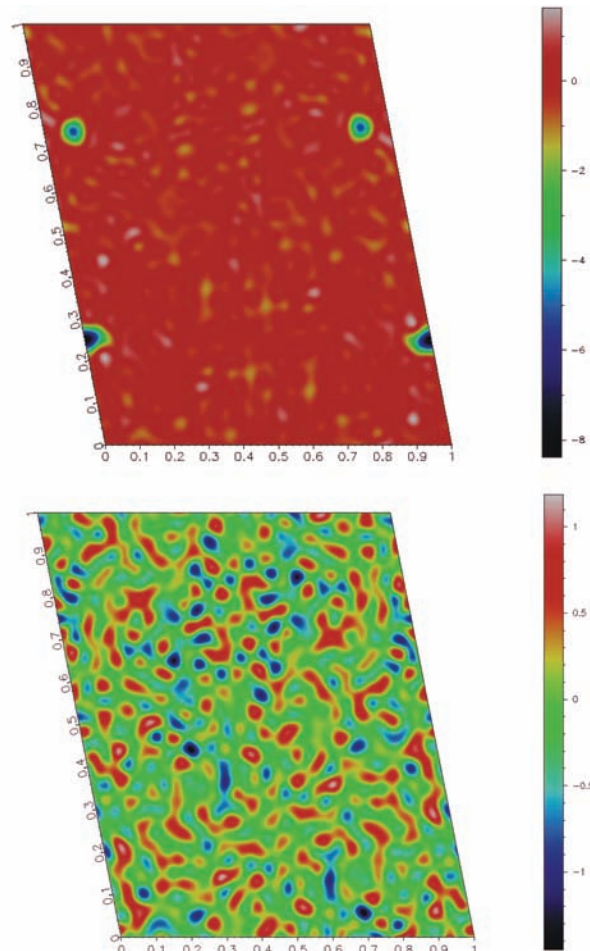


**FIGURE 3.** Difference Fourier maps of the nuclear density (fm/Å<sup>3</sup>) of eudidymite at  $y \sim 0.46$ , (above) before and (below) after the assignment of the H sites. Two intense negative residual peaks at  $x \sim 0.084$ ,  $z \sim 0.745$  and  $x \sim 0.023$ ,  $z \sim 0.251$  (equivalent to  $x \sim -0.023$ ,  $y \sim 0.54$ ,  $z \sim 0.749$ ) are evident before the assignment of the proton sites. Notes: the color scale is different for the two maps; map orientation: x positive to the right.

**TABLE 3A.** Refined positional and thermal displacement parameters ( $\text{\AA}^2$ ) of epididymite

Site	x	y	z	$U_{11}$	$U_{22}$	$U_{33}$	$U_{12}$	$U_{13}$	$U_{23}$	$U_{eq}$
Na	0.10285(12)	0.06934(10)	0.50192(16)	0.0377(6)	0.0220(5)	0.0201(5)	-0.0074(5)	0.0053(5)	-0.0015(4)	0.0266(2)
Be	0.49472(3)	-0.00042(3)	0.34273(5)	0.0068(1)	0.0068(1)	0.0065(1)	0.0005(1)	0.0002(1)	0.0001(1)	0.0067(1)
Si1	0.15908(5)	0.1378(5)	0.01543(9)	0.0040(3)	0.0049(3)	0.0062(3)	-0.0008(2)	0.0001(2)	-0.0002(2)	0.0051(1)
Si2	0.3426(6)	0.13635(5)	0.73115(9)	0.0051(3)	0.0054(3)	0.0059(3)	0.0006(2)	0.0012(2)	-0.0007(2)	0.0054(1)
Si3	0.33173(6)	0.13741(5)	0.30525(10)	0.0065(3)	0.0055(3)	0.0058(3)	0.0010(2)	-0.0017(2)	-0.0002(2)	0.0059(1)
O1	0.12005(7)	1/4	0.00001(13)	0.0136(3)	0.0039(3)	0.0241(4)	0	-0.0031(3)	0	0.0139(1)
O2	0.21704(4)	0.1224(5)	0.21004(8)	0.0084(2)	0.0162(3)	0.0109(2)	-0.0014(2)	-0.0049(2)	0.0005(2)	0.0118(1)
O3	0.06068(4)	0.06612(4)	0.00658(7)	0.0068(2)	0.0077(2)	0.0071(2)	-0.0034(2)	-0.0002(2)	-0.0003(2)	0.0072(1)
O4	0.23777(5)	0.11405(5)	0.84938(9)	0.0108(2)	0.0186(3)	0.0151(2)	-0.0026(2)	0.0078(2)	-0.0021(2)	0.0148(1)
O5	0.43489(4)	0.06457(4)	0.78946(7)	0.0100(2)	0.0093(2)	0.0076(2)	0.0042(2)	0.0004(2)	-0.0006(2)	0.0090(1)
O6	0.37761(7)	1/4	0.76529(12)	0.0133(3)	0.0054(3)	0.0173(4)	0	-0.0032(3)	0	0.0120(1)
O7	0.30497(5)	0.12340(5)	0.52074(7)	0.0120(2)	0.0131(2)	0.0068(2)	0.0019(2)	-0.0009(2)	-0.0002(2)	0.0106(1)
O8	0.37000(7)	1/4	0.26883(12)	0.0124(3)	0.0056(3)	0.0164(3)	0	0.0022(3)	0	0.0115(1)
O9	0.41552(4)	0.06300(4)	0.22624(7)	0.0113(2)	0.0094(2)	0.0077(2)	0.0045(2)	-0.0013(2)	-0.0006(2)	0.0095(1)
OW	0.05713(9)	1/4	0.48974(18)	0.0215(5)	0.0316(6)	0.0333(6)	0	0.0060(5)	0	0.0288(2)
H1	0.00647(21)	1/4	0.58561(43)	0.044(1)	0.051(2)	0.059(2)	0	0.024(1)	0	0.0515(7)
H2	0.01340(27)	1/4	0.38486(45)	0.060(2)	0.060(2)	0.055(2)	0	-0.015(1)	0	0.0586(8)

Notes: The anisotropic displacement factor exponent takes the form:  $-2\pi^2[(ha^*)^2U_{11} + \dots + 2hka^*b^*U_{12}]$ .  $U_{eq}$  is defined as one third of the trace of the orthogonalized  $U_j$  tensor.

**TABLE 3B.** Refined positional and thermal displacement parameters ( $\text{\AA}^2$ ) of eudidymite

Site	x	y	z	$U_{11}$	$U_{22}$	$U_{33}$	$U_{23}$	$U_{13}$	$U_{12}$	$U_{eq}$
Na	0.02899(15)	0.34078(26)	0.92853(13)	0.0256(7)	0.0299(8)	0.0241(7)	-0.0089(6)	0.0089(6)	-0.0102(6)	0.0260(4)
Be	0.16817(5)	0.32317(7)	0.49710(4)	0.0068(2)	0.0058(2)	0.0073(2)	-0.0005(2)	0.0015(2)	0.00050(2)	0.0067(1)
Si1	0.20415(8)	0.01965(13)	0.64127(7)	0.0068(4)	0.0026(3)	0.0047(3)	0.0012(3)	0.0024(3)	-0.0004(3)	0.0045(2)
Si2	0.25166(8)	0.10250(13)	0.86648(7)	0.0058(4)	0.0037(3)	0.0051(3)	0.0010(3)	0.0005(3)	-0.0010(3)	0.0050(2)
Si3	0.02964(8)	0.09397(13)	0.36195(7)	0.0042(4)	0.0062(4)	0.0044(3)	-0.0006(3)	0.0007(3)	-0.0011(3)	0.0050(2)
O1	0.07277(6)	0.03247(11)	0.62614(6)	0.0073(3)	0.0108(3)	0.0148(3)	0.0019(3)	0.0038(2)	-0.0022(2)	0.0108(2)
O2	0.24036(7)	0.18030(11)	0.11540(6)	0.0191(3)	0.0038(3)	0.0159(3)	-0.0004(2)	0.0055(3)	-0.0023(3)	0.0127(2)
O3	0.24045(6)	0.16471(10)	0.57054(5)	0.0087(3)	0.0063(3)	0.0076(3)	0.0030(2)	0.0034(2)	0.0004(2)	0.0073(1)
O4	0.23677(7)	0.43859(12)	0.24484(6)	0.0149(3)	0.0167(3)	0.0051(3)	-0.0022(2)	0.0028(2)	-0.0009(3)	0.0122(2)
O5	0.15480(6)	0.49864(10)	0.05623(6)	0.0083(3)	0.0079(3)	0.0088(3)	0.0032(2)	0.0001(2)	-0.0011(2)	0.0087(1)
O6	0.12854(7)	0.05189(11)	0.87541(6)	0.0080(3)	0.0092(3)	0.0138(3)	0.0010(2)	0.0030(2)	-0.0029(2)	0.0103(1)
O7	0	0.17321(16)	1/4	0.0169(5)	0.0089(4)	0.0064(4)	0	0.0016(4)	0	0.0109(2)
O8	0.05237(6)	0.25694(11)	0.43729(6)	0.0073(3)	0.0108(3)	0.0088(3)	-0.0039(2)	0.0004(2)	-0.0003(2)	0.0092(1)
OW*	0.01209(19)	0.43098(26)	0.74466(21)							0.0241(4)
H1*	0.0840(5)	0.4645(11)	0.7449(4)	0.042(2)	0.083(4)	0.050(3)	-0.001(3)	0.007(2)	-0.018(3)	0.059(2)
H2*	-0.0227(5)	0.5419(7)	0.7486(6)	0.064(5)	0.043(2)	0.055(2)	0.004(3)	0.016(4)	0.020(2)	0.054(2)

\* The site occupancy of OW, H1, and H2 is 50%. The anisotropic displacement factor exponent takes the form:  $-2\pi^2[(ha^*)^2U_{11} + \dots + 2hka^*b^*U_{12}]$ .  $U_{eq}$  is defined as one third of the trace of the orthogonalized  $U_j$  tensor.

Convergence was rapidly achieved and the final least-square cycles were conducted with anisotropic thermal parameters for all sites including the H sites. All the principal mean square atomic displacement parameters were positively defined and the variance-covariance matrix showed no significant correlations among the refined parameters. At the end of the last cycle of refinement, no peak larger than  $+0.9/-0.8 \text{ fm/\AA}^3$  was present in the difference-Fourier map of the nuclear density (Fig. 2; Table 2). The final agreement index ( $R_1$ ) was 0.0317 for 137 refined parameters and 2261 unique reflections with  $F_o > 4\sigma(F_o)$  (Table 2). Positional and displacement parameters are reported in Table 3a. Relevant bond lengths and angles are listed in Table 4a. Table 5<sup>1</sup> has observed and calculated structure factors.

The neutron diffraction data of eudidymite were processed following the same strategy already adopted for epididymite. The preliminary check on the real symmetry of the structure showed that the structure is centrosymmetric at 95.0% likelihood ( $|E^2 - 1| = 0.952$ ) and that space group  $C2/c$  is highly likely (CFOM- $C2/c = 0.490$ ; CFOM- $Cc = 10.070$ ). The anisotropic structure refinement was first performed starting from the atomic coordinates of Fang et al. (1972), without any H sites. When convergence was achieved, two intense negative residual peaks ( $\sim -8 \text{ fm/\AA}^3$ ) at  $x \sim 0.084$ ,  $y \sim 0.465$ ,  $z \sim 0.745$ , and  $x \sim -0.023$ ,  $y \sim 0.542$ ,  $z \sim 0.749$  were found in the final difference-Fourier map of the nuclear density (Fig. 3). Further cycles of least-squares refine-

ment were then performed assigning the H-scattering length to these residual peaks. Convergence was again rapidly achieved and the variance-covariance matrix showed no significant correlations among the refined parameters. All the principal mean square atomic displacement parameters were positively defined; only the oxygen of the water molecules (OW, Table 3b) was kept as isotropic for the reasons explained in the following section. No peak larger than  $+0.9/-0.9 \text{ fm/\AA}^3$  was present in the difference-Fourier map of the nuclear density at the end of the last refinement cycle (Fig. 3; Table 2). The final agreement index ( $R_1$ ) was 0.0478 for 136 refined parameters and 1732 unique reflections with  $F_o > 4\sigma(F_o)$  (Table 2). Positional and displacement parameters are reported in Table 3b. Bond lengths and angles are listed in Table 4b. Observed and calculated structure factors are listed in Table 5<sup>1</sup>.

<sup>1</sup> Deposit item AM-08-037, Table 5 (observed and calculated structure factors). Deposit items are available two ways: For a paper copy contact the Business Office of the Mineralogical Society of America (see inside front cover of recent issue) for price information. For an electronic copy visit the MSA web site at <http://www.minsocam.org>, go to the American Mineralogist Contents, find the table of contents for the specific volume/issue wanted, and then click on the deposit link there.

**TABLE 4A.** Relevant bond distances (Å) and angles (°) in the epididymite structure

Na-O5	2.4492(14)	Be-O9	1.5801(7)	Si1-O3	1.5901(9)	Si2-O5	1.5880(9)	Si3-O9	1.5823(9)
Na-O9	2.4545(14)	Be-O5	1.5845(7)	Si1-O4	1.6116(9)	Si2-O4	1.6213(9)	Si3-O7	1.6306(9)
Na-OW	2.5318(14)	Be-O3	1.6579(7)	Si1-O1	1.6120(8)	Si2-O7	1.6280(9)	Si3-O2	1.6321(9)
Na-O5'	2.6320(14)	Be-O3'	1.6595(7)	Si1-O2	1.6226(9)	Si2-O6	1.6313(8)	Si3-O8	1.6322(8)
Na-O7	2.6806(15)								
Na-O2	2.6898(14)	O9-Be-O5	109.33(4)	O3-Si1-O4	109.61(5)	O5-Si2-O4	110.44(5)	O9-Si3-O7	114.96(5)
Na-O9'	2.9168(15)	O9-Be-O3	114.66(4)	O3-Si1-O1	109.69(5)	O5-Si2-O7	114.03(5)	O9-Si3-O2	111.46(5)
		O9-Be-O3'	112.66(4)	O3-Si1-O2	108.36(5)	O5-Si2-O6	109.96(5)	O9-Si3-O8	109.95(6)
OW-H1	0.955(3)								
OW-H1*	0.987*								
OW...O6	2.909(2)	O5-Be-O3	112.81(4)	O4-Si1-O1	109.21(6)	O4-Si2-O7	104.24(5)	O7-Si3-O2	102.38(5)
H1...O6	1.973(3)	O5-Be-O3'	115.10(4)	O4-Si1-O2	110.99(5)	O4-Si2-O6	108.70(6)	O7-Si3-O8	109.37(6)
OW-H1...O6	166.2(3)	O3-Be-O3'	91.50(3)	O1-Si1-O2	108.96(6)	O7-Si2-O6	109.23(6)	O2-Si3-O8	108.34(6)
OW-H2	0.951(4)								
OW-H2*	0.993*								
OW...O8	3.047(2)								
H2...O8	2.147(4)								
OW-H2...O8	157.6(3)								
H1-OW-H2	101.7(3)								
O6...OW...O8	76.78(4)								

\* Bond distance corrected for "riding motion" following Busing and Levy (1964).

**TABLE 4B.** Relevant bond distances (Å) and angles (°) in the eudidymite structure

Na-O5	2.3918(18)	Be-O8	1.5789(9)	Si1-O3	1.5970(13)	Si2-O5	1.5850(12)	Si3-O8	1.5798(12)
Na-O8	2.4248(20)	Be-O5	1.5837(10)	Si1-O2	1.6109(13)	Si2-O2	1.6219(13)	Si3-O6	1.6246(13)
Na-OW	2.4471(34)	Be-O3	1.6592(10)	Si1-O4	1.6204(12)	Si2-O4	1.6273(13)	Si3-O7	1.6301(11)
Na-OW'	2.6168(34)	Be-O3'	1.6759(9)	Si1-O1	1.6234(13)	Si2-O6	1.6313(13)	Si3-O1	1.6341(13)
Na-O1	2.6346(20)								
Na-O5'	2.6576(21)	O8-Be-O5	109.49(5)	O3-Si1-O2	109.63(7)	O5-Si2-O2	110.49(7)	O8-Si3-O6	114.48(7)
Na-O6	2.6680(21)	O8-Be-O3	113.29(5)	O3-Si1-O4	110.46(7)	O5-Si2-O4	110.10(7)	O8-Si3-O7	109.40(7)
		O8-Be-O3'	114.15(5)	O3-Si1-O1	108.34(7)	O5-Si2-O6	114.09(7)	O8-Si3-O1	112.88(8)
OW-H1	0.940(7)								
OW-H1*	0.988*								
OW...O4	2.993(3)	O5-Be-O3	115.36(5)	O2-Si1-O4	107.85(7)	O2-Si2-O4	108.51(7)	O6-Si3-O7	110.07(7)
H1...O4	2.056(6)	O5-Be-O3'	111.64(5)	O2-Si1-O1	111.07(7)	O2-Si2-O6	103.83(7)	O6-Si3-O1	102.38(7)
OW-H1...O4	174.9(6)								
		O3-Be-O3'	92.11(5)	O4-Si1-O1	109.50(7)	O4-Si2-O6	109.55(7)	O7-Si3-O1	107.25(6)
OW-H2	0.937(6)								
OW-H2*	0.979*								
OW...O7	2.926(2)								
H2...O7	2.120(5)								
OW-H2...O7	143.4(5)								
H1-OW-H2	103.6(7)								
O4...OW...O7	75.59(6)								

Note: For any given Na coordination shell, the Na-OW and Na-OW' bonds are mutually exclusive (see text and Table 3b for details).

\* Bond distance corrected for "riding motion" following Busing and Levy (1964).

## DISCUSSION

This multi-methodological study allowed us to define the correct chemical formula of epididymite and eudidymite and to refine the crystal structures of these two dimorphs to give new insight into the configuration of the extra-framework content.

The chemical analysis shows that a low, but significant, amount of Al and Fe (most likely substituting for Si in the tetrahedral sites) and K (substituting for Na as an extra-framework cation) occurs in both dimorphs. The thermo-gravimetric analysis showed that neither dimorph loses H<sub>2</sub>O up to 805–815 °C, according to the previous experimental findings (Shilin and Semenov 1957).

The refined site positions of the Be/Si-framework for both the minerals are in good agreement with those previously reported by Robinson and Fang (1970) and Fang et al. (1972). As observed in the previous studies, the Be-tetrahedra show two short (~1.58 Å) and two long (~1.66 Å) Be-O bond distances in both the dimorphs. The long bond lengths are those with the O atoms shared by the two tetrahedra of the Be<sub>2</sub>O<sub>6</sub> units (Fig. 1). The anisotropic refinements performed in this study provide a full description

of the thermal motion of framework and extra-framework sites. In addition, the space groups previously reported are here confirmed. A general view of the crystal structures of epididymite and eudidymite, based on the anisotropic refinements of this study, is shown in Figure 4. The analysis of the nuclear-density Fourier maps shows that in both epididymite and eudidymite water molecules are present as extra-framework population, while the presence of hydroxyl groups is unambiguously excluded. On this basis, we infer that the correct chemical formula of the dimorphs is Na<sub>2</sub>Be<sub>2</sub>Si<sub>6</sub>O<sub>15</sub>·H<sub>2</sub>O. Several databases, among those the *American Mineralogist* Crystal Structure Database, report an incorrect chemical formula for epididymite and/or eudidymite of NaBeSi<sub>3</sub>O<sub>7</sub>OH, the reason being that Robinson and Fang (1970) reported the chemical formula of epididymite as NaBeSi<sub>3</sub>O<sub>7</sub>OH, based on the unusually high temperature of dehydration observed for this mineral ( $T > 830$  °C). Open-framework silicates, especially zeolites or zeolite-like minerals, have dehydration temperatures of  $T < 500$  °C. The aforementioned experimental finding led the authors to believe that epididymite contained OH<sup>-</sup> groups, and not H<sub>2</sub>O (Robinson and Fang 1970).

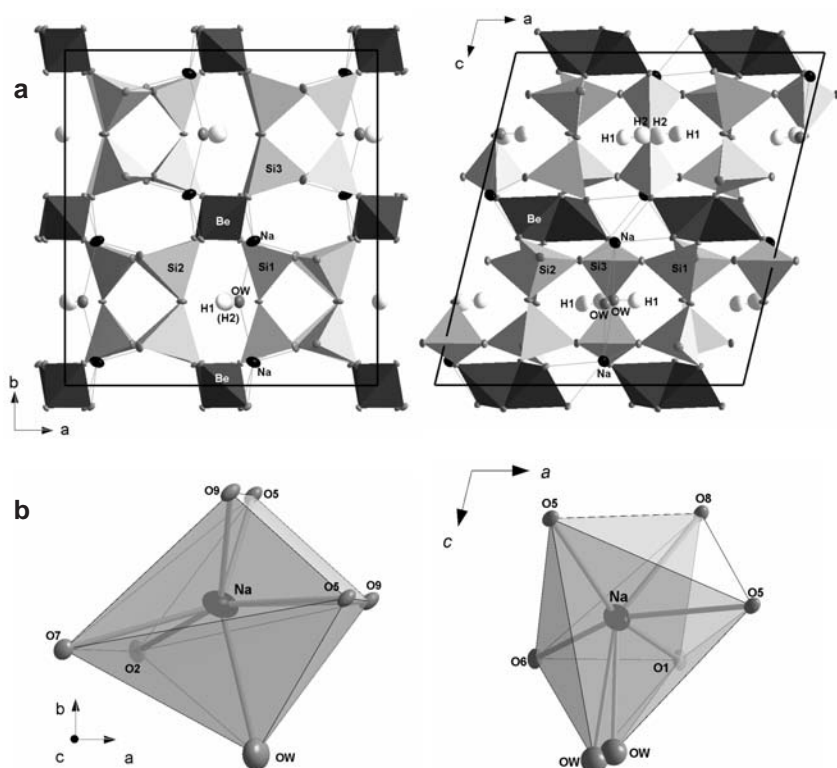


**FIGURE 4.** (a) Crystal structure of (left side) epididymite, viewed down [001], and (right side) eudidymite, viewed down [010], based on the results of this study. Beryllium tetrahedra are in dark gray, Si tetrahedra in light gray. Thermal ellipsoid probability factor: 50%. The OW site is coordinated by two Na sites in both structures. A clearer view of the complex configuration of water molecules in eudidymite is in Figure 5. (b) The coordination polyhedra of Na in (left side) epididymite and (right side) eudidymite.

The geometry of the water molecule and hydrogen bonding in epididymite is now well defined: the OW-H1 and OW-H2 distances, corrected for “riding motion” (Busing and Levy 1964), are  $\sim 0.987$  and  $\sim 0.993$  Å, respectively (Table 4a), and two strong hydrogen bonds to the framework O atoms (H1 $\cdots$ O6  $\sim 1.973$  and H2 $\cdots$ O8  $\sim 2.147$  Å, Table 4a) occur. The H1-OW-H2 angle is unusually low ( $\sim 102^\circ$ , Table 4a), but still in the range of the observed H-O-H angles in solid-state materials (Chiari and Ferraris 1982; Steiner 1998 and references therein). The possible reasons for this “compressed” configuration of the molecule are: (1) the small O6 $\cdots$ OW $\cdots$ O8 value ( $\sim 77^\circ$ , Fig. 5; Table 4a), which forces the H1-OW-H2 angle to decrease to approach linearity in the hydrogen bond, which is energetically less costly (Steiner 1998), and (2) the presence of two Na-OW-Na bonds, as each H<sub>2</sub>O is simultaneously bonded to two different Na sites (i.e., OW acts as bridging O atoms between two Na polyhedra; Fig. 4; Table 4a). The two hydrogen bonds lie on a plane  $\parallel(010)$ , whereas the two Na-OW bonds lie on a plane almost  $\parallel(001)$  (Figs. 4 and 5).

More complex is the configuration of the water molecules and hydrogen bonding in eudidymite. As shown in Figures 4 and 5, two O sites, related by symmetry and mutually exclusive (site occupancy 50%), are only 0.37 Å apart. For this reason, the thermal motion of the OW site was refined as isotropic (Table 3b). Therefore, two statistically distributed configurations of the water molecule occur in the eudidymite structure (Fig. 5). The two O-H bond distances (corrected for riding motion, Busing and Levy 1964) are similar to those in epididymite (OW-H1  $\sim 0.988$  and OW-H2  $\sim 0.979$  Å, respectively; Table 4b), the H1-OW-H2

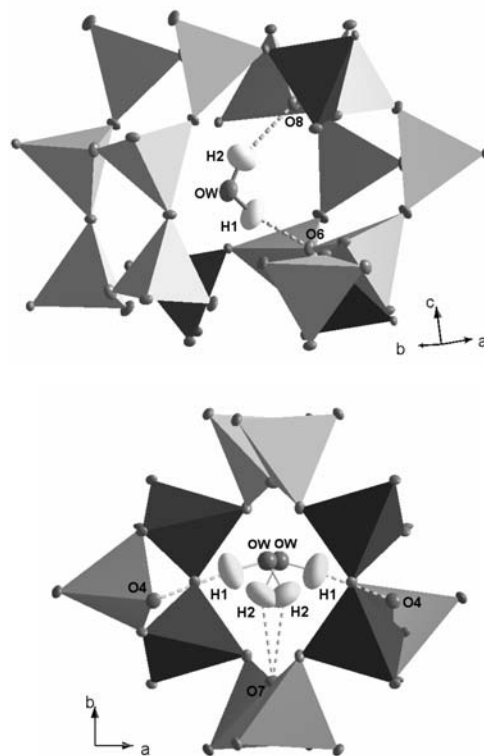


**FIGURE 5.** Configuration of the water molecules and hydrogen bonds in (above) epididymite and (below) eudidymite. Thermal ellipsoid probability factor: 50%.

angle again shows a low but reasonable value ( $\sim 104^\circ$ , Table 4b). Just as for epididymite, the slightly “compressed” configuration of the water molecule in eudidymite is most likely due to the small  $O4 \cdots OW \cdots O7$  value ( $\sim 76^\circ$ , Table 4b) and to the two Na-OW-Na bonds (Fig. 4; Table 4b).

The coordination shells of Na in epididymite and eudidymite are slightly different. Assuming  $Na-O_{\max} < 3 \text{ \AA}$  and  $Na-O_{\max} < Na-Be_{\text{shortest}}$ , the coordination number of the cation in the epididymite structure is  $CN(Na) = 7$  (i.e., six O atoms belonging to tetrahedral framework + one  $H_2O$ ; Table 4a; Fig. 4). In eudidymite,  $CN(Na) = 6$  (five framework O atoms + one  $H_2O$ , Table 4b, Fig. 4). However, the presence of two symmetry-related and partially occupied OW sites (Table 3b), only  $0.37 \text{ \AA}$  apart, leads to two mutually exclusive configurations of the Na polyhedron, statistically distributed by 50% (Fig. 4; Table 4b).

The unusually high temperature of dehydration observed for epididymite and eudidymite observed in this and previous studies (Stavitskaya et al. 1967; Robinson and Fang 1970; Fang et al. 1972, and references therein) is likely due to (1) the peculiar configuration of the water molecule, which is bonded to two Na-sites; (2) to the strong hydrogen bonds to the framework O atoms; and (3) to the small “free diameters” (Baerlocher et al. 2001) of the channels in the tetrahedral framework, which hinder the migration of the water molecules toward the surface of the crystal.

#### ACKNOWLEDGMENTS

The authors thank the Institut Laue-Langevin, Grenoble, France, for the allocation of neutron beam time. The authors are grateful to Mario Picciani, who provided the samples of epididymite and eudidymite used for this study; to Arianna Lopresti for the analyses of BeO and  $H_2O$  performed at Mapei Laboratory; and to Federico Pezzotta of the Museum of Natural History of Milan for the use of the SEM. This study was founded by the Italian Ministry of University and Research, MIUR-Project: 2006040119\_004. The authors thank the Associate Editor Paola Bonazzi, the Technical Editor Andrew Locock, Günther Redhammer, and an anonymous reviewer.

#### REFERENCES CITED

- Baerlocher, Ch., Meier, W.M., and Olson, D.H. (2001) Atlas of zeolite framework types, 5th edition, 302 p. Elsevier, Amsterdam.
- Brögger, W.C. (1890) Die Mineralien der sienitpegmatitgänge der südnorwegischen Augit- und Nephelinsyenite. *Zeitschrift für Kristallographie*, 16, 586–597.
- Busing, W.R. and Levy, H.A. (1964) The effect of thermal motion on the estimation of bond lengths from diffraction measurements. *Acta Crystallographica*, 17, 142–146.
- Černý, P. (1963) Epididymite and milarite-alteration products of beryl from Věžná, Czechoslovakia. *Mineralogical Magazine*, 33, 450–457.
- Chiari, G. and Ferraris, G. (1982) The water molecules in crystalline hydrates studied by neutron diffraction. *Acta Crystallographica*, B38, 2331–2341.
- Coppens, P., Leiserowitz, L., and Rabinovich, D. (1965) Calculation of absorption corrections for camera and diffractometer data. *Acta Crystallographica*, 18, 1035–1038.
- Downs, R.T. and Hall-Wallace, M. (2003) The American Mineralogist crystal structure database. *American Mineralogist*, 88, 247–250.
- Eby, G.N., Roden-Tice, M., Krueger, H.L., Ewing, W., Faxon, E.H., and Woolley, A.R. (1995) Geochronology and cooling history of the northern part of the Chilwa alkaline province, Malawi. *Journal of African Earth Science*, 20, 275–288.
- Fang, J.H., Robinson, P.D., and Ohya, Y. (1972) Redetermination of the crystal structure of eudidymite and its dimorphic relationship to epididymite. *American Mineralogist*, 57, 1345–1354.
- Farrugia, L.J. (1999) WinGX suite for small-molecule single-crystal crystallography. *Journal of Applied Crystallography*, 32, 837–838.
- Flink, G. (1894) Beschreibung eines neuen Mineralfundes aus Grönland. Epididymit. *Zeitschrift für Kristallographie*, 23, 353–358.
- Howard, J.A.K., Johnson, O., Schultz, A.J., and Stringer, A.M. (1987) Determination of the neutron absorption cross section for hydrogen as a function of wavelength with a pulsed neutron source. *Journal of Applied Crystallography*, 20, 120–122.
- Ito, T. (1934) The structure of epididymite ( $HNaBeSi_3O_8$ ). *Zeitschrift für Kristallographie*, 88, 142–149.
- (1947) The structure of eudidymite ( $HNaBeSi_3O_8$ ). *American Mineralogist*, 32, 442–453.
- Larson, A.C. (1970) Crystallographic Computing. F.R. Ahmed, S.R. Hall, and C.P. Huber, Eds., p. 291–294. Munksgaard, Copenhagen, Denmark.
- Lehmann, M.S., Kuhs, W., McIntyre, G.J., Wilkinson, C., and Allibon, J. (1989) On the use of a small two-dimensional position-sensitive detector in neutron diffraction. *Journal of Applied Crystallography*, 22, 562–568.
- Lévy, C.M. (1961) Remarques sur l'épididymite. *Bulletin de la Société Française de Minéralogie*, 84, 320.
- Mandarino, J.A. and Harris, D.C. (1968) Epididymite from Mont St. Hilaire, Quebec. *Canadian Mineralogist*, 9, 706–709.
- Martin, R.F. and De Vito, C. (2005) The patterns of enrichment in felsic pegmatites ultimately depend on tectonic setting. *Canadian Mineralogist*, 43, 2027–2048.
- Nickel, E.H. (1963) Eudidymite from Seal Lake, Labrador, Newfoundland. *Canadian Mineralogist*, 7, 643–649.
- Petersen, O.V. (1966) Crossed axial plane dispersion in epididymite. *American Mineralogist*, 51, 916–919.
- (1994) Some pegmatite minerals from the Zomba district, Malawi. *Mineralogical Record*, 25, 29–38.
- Petersen, O.V., Medenbach, O., and Bollhorn, J. (1997) Epididymite twins. *Neues Jahrbuch für Mineralogie Monatshefte*, 1997(5), 221–228.
- Pobedinskaya, E.A. and Belov, N.V. (1960) The crystal structure of epididymite  $NaBeSi_3O_8(OH)$ : A new type of  $(SiO_4)_n$  chain. *Zhurnal Strukturnoi Khimii*, 1, 51–63.
- Robinson, P.D. and Fang, J.H. (1970) The crystal structure of epididymite. *American Mineralogist*, 55, 1541–1549.
- Secco, L., Guastoni, A., Nestola, F., Redhammer, G.J., and Dal Negro, A. (2007) Crystal chemistry of aegirine as indicator of *P-T* conditions. *Mineralogical Magazine* 71, 249–255.
- Sheldrick, G.M. (1997) SHELX-97. Programs for crystal structure determination and refinement. University of Göttingen, Germany.
- Shilin, L.L. and Semenov, E.I. (1957) Beryllium minerals, epididymite and eudidymite, in alkali pegmatites of the Kola Peninsula. *Doklady Akademii Nauk SSSR*, 112, 325–328.
- Stavitskaya, G.P., Ryskin, Y.I., Kol'tsov, A.I., Shul'gi, E.I., and Pobedonostseva, A.A. (1967). Study of the nature of the hydration of epididymite by means of the infrared absorption spectrum and proton magnetic resonance. *Journal of Structural Chemistry*, 8, 201–205.
- Steiner, T. (1998) Opening and narrowing of the water H-O-H angle by hydrogen-bonding effects: Re-inspection of neutron diffraction data. *Acta Crystallographica*, B54, 464–470.
- Wilkinson, C., Khamis, H.W., Stansfield, R.F.D., and McIntyre, G.J. (1988) Integration of single-crystal reflections using area multidetectors. *Journal of Applied Crystallography*, 21, 471–478.
- Wilson, A.J.C. and Prince, E. (1999) *International Tables for Crystallography*, Volume C. Kluwer Academic Publishers, Dordrecht, The Netherlands.

MANUSCRIPT RECEIVED FEBRUARY 27, 2008

MANUSCRIPT ACCEPTED APRIL 2, 2008

MANUSCRIPT HANDLED BY PAOLA BONAZZI